A calorimetric study on the order-disorder transition of silver ions in $Ag_{0.361}TiS_2$: the two-dimensional nature of the transition

1993 J. Phys.: Condens. Matter 5 6673

(http://iopscience.iop.org/0953-8984/5/36/023)

J. Phys.: Condens. Matter 5 (1993) 6673–6682. Printed in the UK

A calorimetric study on the order–disorder transition of silver ions in $Ag_{0.361}TiS_2$: the two-dimensional nature of the transition

Hiroki Fujimori†, Masaharu Oguni†, Kenzo Kitayama†, Takashi Uchida‡ and Masataka Wakihara‡

† Department of Chemistry, Faculty of Science, Tokyo Institute of Technology, Ookayama-2, Meguro-ku, Tokyo 152, Japan

‡ Department of Chemical Engineering, Faculty of Engineering, Tokyo Institute of Technology, Ookayama-2, Meguro-ku, Tokyo 152, Japan

Received 19 January 1993, in final form 26 April 1993

Abstract. Ag_xTiS_2 intercalation compounds were thermally prepared and characterized by a room-temperature x-ray diffraction method to be of single phases in stage 1, stage 2 and stage 1′ in the ranges $x = 0.36$–0.42, 0.17–0.22 and 0–0.12, respectively. The heat capacities of $Ag_{0.361}TiS_2$ were measured by adiabatic calorimetry in the temperature range between 13 and 400 K. The intralayer order–disorder phase transition of silver ions was observed at 285.5 ± 0.3 K as a higher-order type with wide skirts of anomalous heat capacity on the low- and high-temperature sides of the peak. The enthalpy and entropy of the transition were found to be 4.3 ± 0.4 kJ mol^{-1} and 9.9 ± 1.0 J K^{-1} mol^{-1} (close to R ln 3), respectively, on the assumption of a high-temperature approximation. The interaction of positional ordering of silver ions is suggested to be of a two-dimensional nature, and two theoretical models relevant to the phase transition are discussed.

1. Introduction

Intercalation compounds have attracted interest in recent years [1, 2]. This is because guest atoms or molecules intercalated in a host material show interesting behaviours due to their positional or orientational disordering, and also because new physical properties which do not exist in a host material are produced by the intercalation [3–5]. Graphite and transition-metal dichalcogenides are typical examples of such host materials. The dichalcogenides TX_2 (T=transition metal and X=chalcogen) are made up of layers, each consisting of a plane of metal atoms bounded on both sides by planes of chalcogen atoms. While the atoms within each layer are strongly bonded to each other, the interlayer interaction is relatively weak. The space in between the two adjacent layers is called the van der Waals (VDW) gap, and guest species are intercalated into this gap.

Silver titanium disulphide (Ag_xTiS_2) is an intercalation compound and has received attention on account of its two-dimensional structure, interesting stage transformation [6–8] and high mobility of silver ions [9, 10]. The compositional ranges for stage-1, stage-2 and stage-1′ (with a slightly expanded TiS_2 lattice [6]) single-phase compounds have been reported as $x = 0.35$–0.43, 0.15–0.25 and 0–0.05, respectively [11], and as $x = 0.36$–0.42, 0.19–0.23 and 0–0.09, respectively [9]. For intermediate silver concentrations the relevant two of the stage-1, stage-2 and stage-1′ phases coexist, and the stage-1 compound coexists with metallic silver for $x > 0.43$ [11] or $x > 0.42$ [9].

0953-8984/93/366673+10$07.50

Silver ions in the Ag_xTiS_2 crystal are located at the sites octahedrally surrounded by sulphur ions in the VDW gaps. While the host material, TiS_2, has a hexagonal ($a \times a \times c$) unit cell, the possible sites of silver ions, as shown as points of intersections in figure 1, form a two-dimensional triangular lattice of lattice constant a within the layer. In the stage-1 Ag_xTiS_2 the three-dimensional $\sqrt{3}a \times \sqrt{3}a \times 2c$ superlattice has been observed to exist at low temperatures by x-ray diffraction [9, 12, 13], Raman scattering [14] and electron diffraction experiments [11, 15]. In such a stage-1 compound, the intralayer order–disorder process is potentially described by the lattice gas (Ising) or three-state Potts models as in the systems of He or Kr atoms adsorbed on graphite surfaces [16–19]. Although the structure of the compound is of two-dimensional character, however, a conclusion as to whether the interaction between silver ions is of the two-dimensional nature cannot be made without any relevant data.

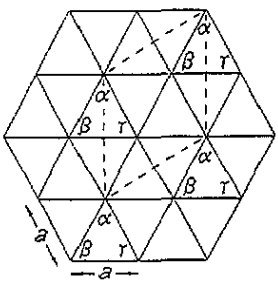

Figure 1. Arrangement of possible Ag sites within a layer. Ag ions are accessible only to the intersection points α, β and γ. When $x = 1$, all the sites are occupied. When $x = 0.33$, only α sites are occupied at low temperatures, and the $\sqrt{3}a \times \sqrt{3}a$ Ag superlattice (– – –) is formed. a corresponds to a lattice constant of the TiS_2 host structure.

Jackle and Irwin [20] investigated the transition using differential scanning calorimetry (DSC) and pointed out that the transition was of the second order based on no observation of any detectable hysteresis effect and of a quasi-two-dimensional system of the intercalated atoms based on the heat-capacity curve obtained compared with a two-dimensional Ising model [21]. With DSC, however, it is too difficult to determine the baseline in estimating the temperature dependence of the anomalous part of the heat capacity. Their result of the estimation in fact seems to be rather small in the total anomaly and narrow in the temperature range, and thus the nature of the transition, which has never been examined in detail, is worth reinvestigation using data of high quality.

In the present study, firstly the stage structure of Ag_xTiS_2 is characterized as a function of silver ion concentration x, leading to the determination of minimum x of the stage-1 Ag_xTiS_2 as employed for heat-capacity measurements. Then the intralayer order–disorder transition of silver ions in the stage-1 compound is examined calorimetrically and its nature is discussed in comparison with that in another typical intercalation compound of graphite, and with the theoretical results of two-dimensional Ising and three-state Potts models [21, 22].

2. Experimental details

Titanium disulphide was first prepared according to the paper of McKelvy and Glaunsinger [23]. Titanium (100 mesh) and crystalline sulphur powders, both purchased from Soekawa Chemicals Co. Ltd, had nominal purities of 99.99% and 99.999%, respectively. The composition of the gold-coloured $Ti_{1+x}S_2$ obtained was determined to be $Ti_{1.006\pm0.001}S_2$ by thermogravimetric analysis in which the $Ti_{1+x}S_2$ was oxidized to TiO_2 at 1000 °C in air. The lattice parameters were found by the x-ray diffraction method described later to be $a_0 = 3.408 \pm 0.003$ Å and $c_0 = 5.696 \pm 0.004$ Å in the hexagonal lattice in agreement with the values in the literature [23].

The intercalation of silver into TiS_2 was achieved by direct reactions of Ag and TiS_2. Silver powder (325 mesh), which was purchased from Aldrich Chemical Company, had a nominal purity of 99.99%. Ag and TiS_2 powders of the desired composition ratios ($0 < x \leqslant 0.45$) were mixed in an agate mortar and allowed to react in an evacuated quartz ampoule. The ampoules were heated either at 1000 °C for 6 d or at 400 °C for 3 weeks and then were cooled slowly to room temperature by leaving the furnace turned off. After cooling, no excess sulphur was found. The stage-1, stage-2 and stage-1′ (confirmed later by an x-ray diffraction method) silver-intercalated powders were black, black–green and gold–green, respectively, with a clear difference from TiS_2 which was a gold colour. The crystal sizes of the powder sample were found by microscopic observation to be of the order of micrometres.

Powder x-ray diffraction patterns of Ag_xTiS_2 samples with $x = 0$–0.45 were obtained at room temperature using a Jeol JDX-7E x-ray powder diffractometer with nickel-filtered Cu Kα radiation. The diffraction spectra were collected in the 2θ range between 5° and 70°.

The heat capacities of $Ag_{0.361}TiS_2$, which was prepared at 1000 °C, were measured with an adiabatic calorimeter described elsewhere [24]. The specimen was loaded into a calorimeter cell together with helium gas at 10^5 Pa to help with heat conduction. The mass of specimen employed was found by a weighing method to be 17.413 g (corresponding to 0.11508 mol). A platinum-resistance thermometer (Minco Products S1059, USA), which had been calibrated on an ITS-90 [25], was used. The heat-capacity measurements were carried out in the temperature range 13–400 K, and their inaccuracies were previously found to be within ±0.3% and ±0.2% below and above 35 K, respectively [24].

3. Results and discussion

3.1. Characterization of Ag_xTiS_2 crystals by means of room-temperature x-ray diffraction

Some typical examples of the x-ray diffraction patterns obtained for Ag_xTiS_2 ($x = 0$–0.45), which had been synthesized at 1000 °C, are depicted in figure 2. The hexagonal lattice parameters a_0 and c_0 were calculated from these patterns. In this figure the numbers in parentheses after the Miller indices (hkl) denote the stage.

The x regions where single-phase compounds were synthesized were also determined from these patterns: that is, the stage-1′ phase was formed for $0 < x < 0.12$, the stage-2 phase for $0.17 < x < 0.22$ and the stage-1 phase for $0.36 < x < 0.42$. This result is in reasonable agreement with those of Scholz and Frindt [11] and Gerards *et al* [9].

The lattice parameter c_0 divided by the stage number n is plotted as a function of x in figure 3. The open squares represent $\frac{1}{2}c_0$ of the compounds with the stage-2 structure while the open circles represent c_0 of the compounds with the stage-1 structure. c_0 for the stage-1′ single phase ($0 < x < 0.12$) increases monotonically with increasing x, exhibiting a striking contrast to the behaviour of c_0 which remains almost constant in the stage-1 or stage-2 single phases.

Figure 4 shows the plots of the intensity ratios of particular diffraction peaks to determine the minimum x in the stage-1 single phase. The open squares represent the ratio $I_{002(1)}/I_{001(1)}$ against x referred to the scale of the right-hand side ordinate. As the amount of intercalated silver atoms increases, $I_{002(1)}$ should increase while $I_{001(1)}$ should decrease, leading to an accelerated increase in the ratio. The ratio increased with increasing x gently up to $x = 0.36$ and steeply above $x = 0.36$, exhibiting a definite bend at this x-value. The full circles in the figure, referred to the scale of the left-hand side ordinate,

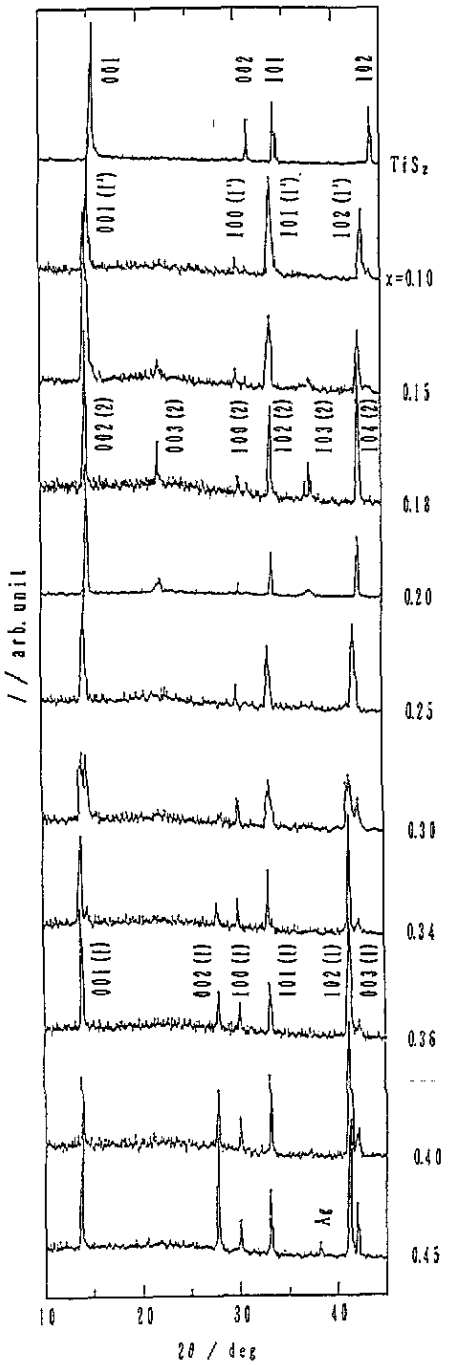

Figure 2. X-ray diffraction patterns of Ag_xTiS_2 powder crystals. The value of x is written on the right-hand side.

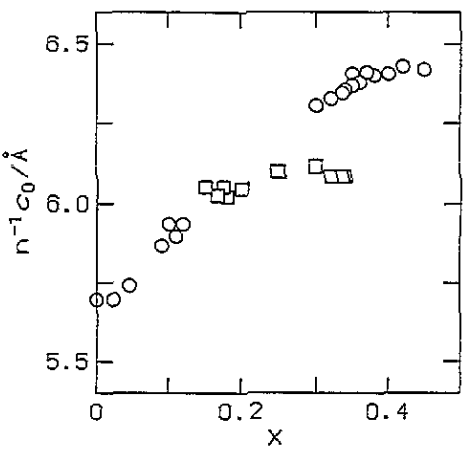

Figure 3. The lattice parameter c_0 of Ag_xTiS_2: ○, stage 1; □, stage 2. n represents the stage number.

represent the ratio $I_{002(2)}/(I_{001(1)} + I_{002(2)})$ which is interpreted to represent the fraction of stage-2 compound coexisting with the stage-1 compound. The plots give almost a straight-

line dependence on x; the extrapolation indicates that the lower compositional end of the stage-1 phase is $x = 0.36$. Thus the minimum x in the stage-1 single phase is determined to be 0.36 ± 0.01 from the results of both ratios.

The same phase relations were obtained for both sets of samples which were synthesized by holding the TiS_2 and Ag mixture at 400 °C for 3 weeks or at 1000 °C for 6 d.

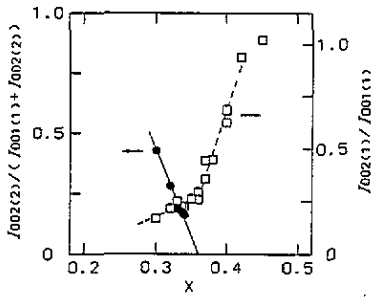

Figure 4. x dependence of the intensity ratio of x-ray diffraction spectra: ●, $I_{002(2)}/(I_{001(1)} + I_{002(2)})$, indicating the fraction of the region with stage-2 structure in each crystal; □, $I_{002(1)}/I_{001(1)}$, related to the amount of silver ions intercalated between TiS_2 layers; —, – – –, guides for the eye.

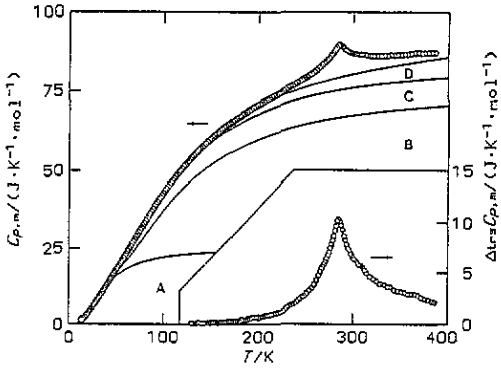

Figure 5. Molar heat capacities of $Ag_{0.361}TiS_2$ and the heat-capacity curves separated into the contributions from each kind of degree of freedom: curve A, lattice vibration; curve B, TiS_2-interlayer local vibration; curve C, silver-related local vibration; curve D, $C_p - C_v$ correction. The inset shows the excess anomalous heat capacities due to the rearrangement of intercalated silver ions.

3.2. Heat capacities

The molar heat capacities obtained for $Ag_{0.361}TiS_2$ are given in table 1 and shown in figure 5 graphically. No anomalous temperature drift nor temperature hysteresis effect was observed over the total temperature range of measurements. Standard thermodynamic functions were derived from the data and are summarized in table 2. The heat-capacity values below 13 K were then estimated by extrapolating the data in terms of AT^3 as a low-temperature approximation of the Debye function with $A = 5.816 \times 10^{-4}$ J K^{-4} mol^{-1}. The entropy at 298.15 K was evaluated to be 101.9 ± 0.3 J K^{-1} mol^{-1}.

The normal heat capacity of $Ag_{0.361}TiS_2$, except for the contribution due to the relevant degree of freedom of the rearrangement of silver ions, was approximated to be composed of the contributions from three degrees of lattice-vibrational freedom, six degenerate degrees of TiS_2-intralayer local-vibrational freedom, $3x$ degenerate degrees of silver-related local-vibrational freedom, and a $C_p - C_v$ correction term. The first (i.e. lattice vibrational) contribution was estimated using the Debye approximation. The TiS_2-intralayer local vibrations were recognized as titanium-related local modes of vibration and assumed to be degenerate by six degrees of freedom on the consideration of actual equivalency of six sulphur atoms surrounding the titanium atom. The same consideration was applied to the silver-related local modes of vibration. These two contributions were calculated by use of the Einstein function. The last (i.e. $C_p - C_v$) correction term is often approximated by the expressions

$$C_p - C_v = \alpha^2 V_m T/\beta \simeq AC_p^2 T$$

Table I. Molar heat capacities of $Ag_{0.361}TiS_2$; $R = 8.31451\ J\ K^{-1}\ mol^{-1}$.

T_{av} (K)	$C_{p,m}/R$	T_{av} (K)	$C_{p,m}/R$	T_{av} (K)	$C_{p,m}/R$	T_{av} (K)	$C_{p,m}/R$
14.00	0.1920	71.04	3.455	158.04	7.502	272.23	10.20
14.70	0.2174	72.53	3.543	160.02	7.559	273.54	10.25
15.42	0.2452	74.01	3.634	162.01	7.622	274.85	10.29
16.15	0.2744	75.51	3.724	164.02	7.676	276.16	10.36
16.93	0.3085	77.00	3.814	166.05	7.731	277.48	10.42
17.76	0.3452	78.50	3.907	168.09	7.786	278.79	10.48
18.67	0.3864	80.00	3.997	170.14	7.841	280.12	10.54
19.66	0.4327	81.50	4.086	172.21	7.891	281.44	10.62
20.73	0.4845	83.02	4.174	174.29	7.943	282.76	10.68
21.87	0.5424	84.53	4.263	176.39	7.997	284.09	10.76
23.05	0.6049	86.05	4.354	178.51	8.039	285.42	10.79
24.16	0.6610	87.58	4.440	180.64	8.091	286.75	10.78
25.15	0.7142	89.12	4.525	182.79	8.160	288.09	10.74
26.47	0.7870	90.66	4.622	184.96	8.198	289.44	10.70
27.45	0.8404	92.20	4.707	187.14	8.244	290.80	10.64
28.43	0.8934	93.76	4.791	189.34	8.304	292.16	10.60
29.42	0.9470	95.32	4.878	191.56	8.352	293.52	10.56
30.40	1.002	96.89	4.961	193.79	8.407	294.90	10.53
31.38	1.059	98.46	5.047	196.03	8.450	296.28	10.52
32.36	1.118	100.05	5.134	198.28	8.495	297.67	10.49
33.33	1.175	101.64	5.218	200.55	8.531	299.06	10.47
34.29	1.232	103.24	5.300	202.83	8.582	300.46	10.45
35.25	1.286	104.86	5.383	205.13	8.631	301.87	10.45
36.20	1.341	106.48	5.467	207.44	8.682	303.28	10.45
37.19	1.398	108.10	5.548	209.76	8.717	304.70	10.44
38.24	1.460	109.74	5.627	212.10	8.766	306.12	10.42
39.33	1.522	111.38	5.704	214.45	8.807	307.54	10.42
40.43	1.585	113.04	5.786	216.81	8.853	308.98	10.43
41.52	1.650	114.70	5.867	219.18	8.895	310.41	10.43
42.62	1.714	116.37	5.946	221.57	8.942	312.83	10.40
43.72	1.777	118.05	6.024	223.98	8.973	314.72	10.38
44.83	1.841	119.73	6.101	226.39	9.025	318.17	10.37
45.96	1.905	121.43	6.186	228.82	9.084	321.63	10.37
47.10	1.971	123.14	6.251	231.26	9.143	325.10	10.37
47.88	2.019	124.86	6.326	233.72	9.194	328.59	10.36
48.71	2.071	126.59	6.399	236.19	9.240	332.09	10.37
49.98	2.149	128.33	6.473	238.67	9.284	335.61	10.37
51.25	2.229	130.08	6.551	241.17	9.341	339.14	10.40
52.52	2.308	131.84	6.619	243.67	9.398	342.69	10.38
53.80	2.386	133.62	6.682	246.20	9.453	346.25	10.39
55.07	2.464	135.41	6.754	248.73	9.495	349.81	10.41
56.35	2.543	137.22	6.829	251.27	9.557	353.38	10.42
57.63	2.621	139.04	6.893	253.83	9.619	356.97	10.42
58.92	2.697	140.87	6.952	256.40	9.674	360.57	10.45
60.20	2.781	142.72	7.016	258.98	9.745	364.18	10.47
61.18	2.836	144.59	7.083	261.57	9.825	367.80	10.48
62.15	2.902	146.47	7.147	263.99	9.907	371.44	10.47
63.63	2.996	148.36	7.207	265.73	9.965	375.08	10.47
65.11	3.089	150.27	7.267	267.02	10.02	378.74	10.49
66.59	3.181	152.19	7.333	268.32	10.06	382.36	10.49
68.08	3.273	154.12	7.392	269.62	10.10	385.95	10.50
69.56	3.364	156.07	7.447	270.92	10.14		

Table 2. Standard thermodynamic functions of $Ag_{0.361}TiS_2$; $R = 8.31451$ J K^{-1} mol^{-1}.

T (K)	$C^\circ_{p,m}/R$	$\Delta_0^T H^\circ_m/R$ (K)	$\Delta_0^T S^\circ_m/R$	Φ°_m/R	T (K)	$C^\circ_{p,m}/R$	$\Delta_0^T H^\circ_m/R$ (K)	$\Delta_0^T S^\circ_m/R$	Φ°_m/R
0	0	0	0	0	200	8.531	936.0	8.450	3.770
10	0.070	0.175	0.023	0.006	210	8.724	1022	8.871	4.003
20	0.449	2.558	0.173	0.045	220	8.908	1110	9.281	4.234
30	0.980	9.651	0.454	0.132	230	9.108	1201	9.681	4.462
40	1.561	22.36	0.815	0.256	240	9.320	1293	10.07	4.687
50	2.150	40.88	1.226	0.409	250	9.527	1387	10.46	4.910
60	2.766	65.47	1.673	0.582	260	9.779	1483	10.84	5.131
70	3.391	96.28	2.147	0.771	270	10.11	1583	11.21	5.349
80	3.996	133.2	2.639	0.974	280	10.54	1686	11.59	5.565
90	4.580	176.1	3.144	1.187	290	10.67	1793	11.96	5.780
100	5.131	224.7	3.655	1.408	298.15	10.48	1879	12.26	5.953
110	5.640	278.6	4.168	1.636	300	10.46	1898	12.32	5.992
120	6.113	337.4	4.679	1.868	310	10.42	2003	12.66	6.201
130	6.543	400.7	5.186	2.104	320	10.37	2107	12.99	6.408
140	6.924	468.1	5.685	2.342	330	10.37	2210	13.31	6.613
150	7.261	539.0	6.175	2.581	340	10.39	2314	13.62	6.814
160	7.562	613.2	6.653	2.821	350	10.40	2418	13.92	7.013
170	7.834	690.2	7.120	3.060	360	10.45	2522	14.22	7.209
180	8.082	769.8	7.575	3.298	370	10.47	2627	14.50	7.403
190	8.315	851.8	8.018	3.535	380	10.49	2732	14.78	7.593

where α, β and V_m are the thermal expansivity, isothermal compressibility and molar volume, respectively, and A is some compound-dependent constant [26]. Since neither α nor β was known at all, the last expression was employed. With θ_D, $\theta_E(TiS_2)$, $\theta_E(Ag)$ and A as adjustable parameters, the observed heat capacities were fitted by the function

$$C_p(T) = C_D(T) + C_{E,Ti}(T) + C_{E,Ag}(T) + AC_p^2T.$$

The data in the temperature range 13–120 K were used for the fitting. The values of parameters derived were the same even if the temperature range in the fitting was changed from 120 to 150 K. The derived parameters θ_D, $\theta_E(TiS_2)$, $\theta_E(Ag)$ and A were 161 K, 400 K, 261 K and 2.20×10^{-6} J^{-1} mol, respectively, and the contributions to the heat capacity are depicted in figure 5 as the portions divided by full curves.

With the normal part of the heat capacity (baseline) determined above, the anomalous part of the heat capacity can be derived by subtracting the baseline from the observed value and is plotted as an inset in figure 5. The heat capacity is in principle due only to the contribution from the degree of freedom of the rearrangement of silver ions, namely the degree of freedom associated with the phase transition in Ag_xTiS_2. The phase transition temperature T_{trs} was found to be 285.5 ± 0.3 K. The curve exhibits skirts over wide temperature ranges on both sides of the transition temperature. The width appears to be much larger than that in the DSC result [20]. On the assumption that the anomalous heat capacity above 400 K had the temperature dependence BT^{-2} as the leading term of the high-temperature expansion in many simple models, the enthalpy and entropy of transition were evaluated to be 4.3 ± 0.4 kJ Ag-mol^{-1} and 9.9 ± 1.0 J K^{-1} Ag-mol^{-1}, respectively.

The x-ray diffraction studies [9, 12, 13] have shown that the low-temperature phase of the stage-1 crystal has the arrangement of silver ions of a $\sqrt{3}a \times \sqrt{3}a$ superlattice in a layer. Provided that each silver ion is restricted in one $\sqrt{3}a \times \sqrt{3}a$ unit cell even in the completely disordered state, i.e. the ion is accessible only to the three sites α, β and γ within a cell (see figure 1), the transition entropy per 1 mol of silver ions is equal

to $R \ln 3 = 9.13\ \mathrm{J\ K^{-1}\ mol^{-1}}$. This value is quite close to the present observation of $9.9 \pm 1.0\ \mathrm{J\ K^{-1}\ mol^{-1}}$. The real situation of the transition in the temperature range measured is thus considered to be almost the same as provided above.

3.3. Quantitative examination of the nature of the phase transition due to rearrangement of silver ions

The phase transition with heat-capacity peak at 285.5 ± 0.3 K was understood to be essentially the process that each silver ion takes the site specified with the $\sqrt{3}a \times \sqrt{3}a$ superlattice, say the α site, in the ordered state, while the three sites within the $\sqrt{3}a \times \sqrt{3}a$ 'unit lattice', the α, β and γ sites in figure 1, with the same probabilities of $\frac{1}{3}$ in the disordered state. Such processes have been found in gas systems adsorbed by a third of the accessible sites on graphite surfaces [16–19], graphite intercalation compounds (GICs) such as C_6Li [27] and so on. The nature of those phase transitions has been considered with reference to three-state Potts models taking only nearest-neighbour interactions into account; that is, the transition is of the first order in the case of three-dimensional interaction systems while of the second order in the two-dimensional systems [28,29]. The anomalous part of the heat capacity per mole of silver ions is plotted in figure 6 where the full and broken (short dashes) curves represent the theoretical curves of the three-state Potts model on a two-dimensional square lattice [22] and on a three-dimensional cubic lattice [30], respectively, by a Monte Carlo simulation. Replacement of the square lattice by the triangular lattice relevant to the present compound would not make a large difference in the theoretical curve, as known in the cases of two-dimensional Ising systems [31–33]. In the three-dimensional case, in addition to the characters of the first-order transition such as a temperature hysteresis effect and a latent heat, the shape of the heat-capacity curve shows little fluctuational effect on the high-temperature side of the peak. The temperature dependence of the anomalous heat capacity derived at present, without any sign of the first-order transition, is definitely close to the theoretical curve in the two-dimensional case. This suggests that the interaction dominating the positional ordering–disordering of silver ions is of a two-dimensional nature with a considerably weakened interlayer interaction through the TiS_2 layer.

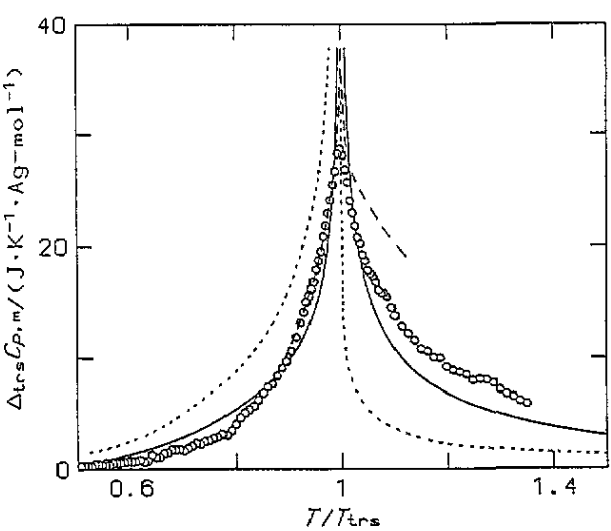

Figure 6. Temperature dependence of the anomalous heat capacities of $Ag_{0.361}TiS_2$ per mole of silver ions: —, heat-capacity curve derived by Monte Carlo simulations for the three-state Potts model on a two-dimensional square lattice [22]; ----, heat-capacity curve derived by Monte Carlo simulations for the three-state Potts model on a three-dimensional cubic lattice [30]; — — —, heat-capacity curve for the Ising model with 0.350 occupancy fraction on a two-dimensional triangular lattice [21].

In the scheme of the Potts model, however, each silver ion is restricted in its position to within a set of α, β and γ sites in figure 1 even in the high-temperature disordered state.

Such a restriction may not be applied *a priori* to the present system. This consideration leads to a two-dimensional lattice gas (Ising) model (with occupancy fraction of about $\frac{1}{3}$) on a triangular lattice as a more appropriate model in a quantitative sense than the above. The broken (long dashes) curve in figure 6 represents the theoretical curve of the model taking only the nearest-neighbour repulsive interactions into consideration with 0.350 occupancy fraction [21]. The heat capacities on the high-temperature side of the transition point are much larger than those of the two-dimensional Potts model. This clearly reflects the difference between the situations with and without the above restriction. The entropy of transition, being correspondingly different between the two models, is much larger for the Ising model than R ln 3 for the three-state Potts model. The experimental data are well on the curve of the Ising model at low temperatures, but in between those of the two models at high temperatures. The experimental entropy of transition was estimated above on the assumption of the high-temperature approximation to be larger than R ln 3. It follows that the phase transition of the present system should be described by the lattice gas (Ising) model in the strict sense, but for the description of the real situation by the model especially at high temperatures the expression for the Hamiltonian would need to be modified to include the second- or further-distant-neighbour attractive interactions in addition to the nearest-neighbour interactions. This would be closely connected with the fact that the lower limit of composition in the stage-1 single-phase structure was found to be 0.36 and not 0.33 at room temperature.

The experimental heat capacities at around the transition point show a rounding effect compared with the theoretical curves. The effect is considered to have been caused by the presence both of the distribution in particle sizes of the powder crystals and of a minute quantity of Ti ions as impurities intercalated between TiS_2 layers, since the presence of a small distribution in the transition temperatures would yield a severe rounding effect on the heat-capacity peak. However, the heat capacities, as have been discussed above in this section, in the temperature range far from the transition point are expected to be affected very little by the presence of the distribution in the transition temperatures.

Here it is of interest to compare the properties of Ag_xTiS_2 intercalation compounds with those of lithium graphite intercalation compounds (Li GICs) because, in the stage-1 LiGIC (C_6Li), lithium ions occupy the sites on the $\sqrt{3}a \times \sqrt{3}a$ in-plane superlattice in the ordered state and their order–disorder process is represented approximately by the three-state Potts model as well [34]. Ag_xTiS_2 crystals showed stacking structures for only stage 1 and stage 2, and the system of positional order–disorder phase transition of silver ions in stage-1 Ag_xTiS_2 was suggested above to be characteristic of the two-dimensional model on a triangular lattice. On the other hand, LiGIC crystals exhibit stage-n stacking structures with $n \geqslant 3$ in addition to $n = 1$ and 2 [35–37], and the order–disorder transition in C_6Li is, quite similarly to the result of the Monte Carlo simulation for the three-dimensional three-state Potts model [30], of first-order nature showing a discontinuous jump in the configurational state, a temperature hysteresis effect of about 5 K, and no marked heat-capacity skirt on the high-temperature side of the transition point [27]. Thus one can see quite a contrast between the analogous intercalation compounds Ag_xTiS_2 and LiGIC, due to difference between the two-dimensional natures of their interactions associated with the positional ordering–disordering of intercalants.

4. Concluding remarks

The present study indicated that the interaction between intercalants in their positional ordering–disordering is of a strongly two-dimensional nature in the stage-1 intercalation

compound Ag_xTiS_2 while it is of a three-dimensional nature in GICs. In this respect, the differences observed between the phase transition behaviours of the two compounds as the amounts of intercalants decrease naturally are of interest. It would be expected that the amount of intercalant would have little effect on behaviour such as the transition temperature and the anomalous heat capacity per mole of intercalants for Ag_xTiS_2, and a marked effect for GICs. This constitutes part of our research which is now under investigation in our laboratory.

Acknowledgments

One of the authors (M Oguni) thanks the Nippon Sheet Glass Foundation for Materials Science for partial financial support of this work.

References

[1] Legrand A P and Flandrois S (ed) 1987 *Chemical Physics of Intercalation (NATO ASI Series B 172)* (New York: Plenum)
[2] Luders K and Schollhorn R (ed) 1989 *Graphite Intercalation Compounds (Synth. Met. 34)*
[3] Whittingham M S 1976 *Science* **192** 1126; 1979 *J. Solid State Chem.* **29** 303
[4] Negishi H, Shoube A, Takahashi H, Ueda Y, Sasaki M and Inoue M 1987 *J. Magn. Magn. Mater.* **67** 179
[5] Satoh T, Tazuke Y, Miyadai T and Hoshi K 1985 *J. Phys. Soc. Japan* **54** 2088
[6] Bardhan K K, Kirczenow G, Jackle G and Irwin J C 1986 *Phys. Rev.* B **33** 4149
[7] Burr G L, Young V G Jr, McKelvy M J, Glaunsinger W S and von Dreele R B 1990 *J. Solid State Chem.* **84** 355
[8] Zhou O, Fischer J E and Liang K S 1991 *Phys. Rev.* B **44** 7243
[9] Gerards A G, Roede H, Haange R J, Boukamp B A and Wiegers G A 1984–5 *Synth. Met.* **10** 51
[10] Kaluarachchi D and Frindt R F 1985 *Phys. Rev.* B **31** 3648
[11] Scholz G A and Frindt R F 1980 *Mater. Res. Bull.* **15** 1703
[12] Wiegers G A, Bronsema K D, van Smaalen S, Haange R J, Zondag J E and de Boer J L 1987 *J. Solid State Chem.* **67** 9
[13] Suter R M, Shafer M W, Horn P M and Dimon P 1982 *Phys. Rev.* B **26** 1495
[14] Leonelli R, Plischke M and Irwin J C 1980 *Phys. Rev. Lett.* **45** 1291
[15] Rajora O S and Curzon A E 1988 *Thin Solid Films* **164** 81
[16] Tejwani M J, Ferreira O and Vilches O E 1980 *Phys. Rev. Lett.* **44** 152
[17] Bretz M 1977 *Phys. Rev. Lett.* **38** 501
[18] Bretz M, Dash J D, Hickernell D C, McLean E O and Vilches O E 1973 *Phys. Rev.* A **8** 1589
[19] Berker A N, Ostlund S and Putnam F A 1978 *Phys. Rev.* B **17** 3650
[20] Jackle G and Irwin J C 1988 *J. Phys. C: Solid State Phys.* **21** 17
[21] Schik M, Walker J S and Wortis M 1977 *Phys. Rev.* B **16** 2205
[22] Binder K 1981 *J. Stat. Phys.* **24** 69
[23] McKelvy M J and Glaunsinger W S 1986 *Mater. Res. Bull.* **21** 835; 1987 *J. Solid State Chem.* **66** 181
[24] Fujimori H and Oguni M 1993 *J. Phys. Chem. Solids* **54** 271
[25] Preston-Thomas H 1990 *Metrologia* **27** 3
[26] Nernst V W and Lindemann F A 1911 *Z. Elektrochem.* **18** 817
[27] Rossat-Mignod J, Wiedenmann A, Woo K C, Milliken J W and Fischer J E 1982 *Solid State Commun.* **44** 1339
[28] Potts R B 1952 *Proc. Camb. Phil. Soc.* **48** 106
[29] Wu F Y 1982 *Rev. Mod. Phys.* **54** 235
[30] Wilson W G and Vause C A 1987 *Phys. Rev.* B **36** 587
[31] Onsager L 1944 *Phys. Rev.* **65** 117
[32] Houtappel R M F 1950 *Physica* **16** 425
[33] Newell G F 1950 *Phys. Rev.* **79** 876
[34] Bak P and Domany E 1979 *Phys. Rev.* B **20** 2818
[35] Bagouni M, Guérard D and Hérold A 1966 *C. R. Acad. Sci., Paris* C **262** 557
[36] Billaud D, McRae E and Hérold A 1979 *Mater. Res. Bull.* **14** 857
[37] Pfluger P, Geiser V, Stolz S and Güntherodt H J 1981 *Synth. Met.* **3** 27